Computational fluid dynamic prediction of the residence time distribution of a prototype hydrodynamic vortex separator operating with a base flow component

D. A. Egarr, M. G. Faram, T O'Doherty, D. A. Phipps and N Syred

Proceedings of the Institution of Mechanical Engineers, Part E: Journal of Process Mechanical Engineering 2005 219: 53
DOI: 10.1243/095440805X7017

Computational fluid dynamic prediction of the residence time distribution of a prototype hydrodynamic vortex separator operating with a base flow component

D A Egarr[1]*, M G Faram[2], T O'Doherty[1], D A Phipps[3], and **N Syred[1]**
[1]Department of Mechanical Engineering, Cardiff University, Cardiff, UK
[2]Hydro International plc, Clevedon, Somerset, UK
[3]Department of Biomolecular Sciences, Liverpool John Moores University, Liverpool, UK

The manuscript was received on 1 March 2004 and was accepted after revision for publication on 11 August 2004.

DOI: 10.1243/095440805X7017

Abstract: A hydrodynamic vortex separator (HDVS) has been modelled using computational fluid dynamics (CFD) in order to accurately determine the residence time of the fluid at the two outlets of the HDVS using a technique that was developed for use in heating, ventilation, and air conditioning (HVAC). The results have been compared with experimental data [**1**]. It is shown that, in using CFD, it is possible to study the response to a variety of inputs, and also to determine the mean residence time of the fluid within the separator. Although the technique used for determining the residence time was developed for use in HVAC, it is shown here to be applicable for the analysis of hydraulic systems, specifically, wastewater treatment systems.

Keywords: computational fluid dynamics (CFD), residence time, hydrodynamic vortex separator, combined sewer overflow

1 INTRODUCTION

1.1 Background

The oldest and most traditional forms of urban drainage are combined sewers, whereby storm and surface water as well as foul wastes are transported to sewage works in the same pipeline. A problem with this system is that, during or after a storm where the quantity of water being passed through the system exceeds the design limit, combined sewer overflows (CSOs) are required, which pass polluting water and organic material into the receiving water course, such as a river.

A method used to reduce the frequency and magnitude of a spill is the 'storage chamber' which is essentially a tank used to hold a large quantity of water until the storm load subsides. An inherent problem with storage chambers, however, is that sedimentation takes place, dictating a maintenance commitment. Spill events can still take place when a very large storm occurs that exceeds the design of the storage chamber, with the consequence of polluting the receiving water course.

Another type of drainage system adopted in regions such as the United States is the provision of a 'sanitary sewer' which carries domestic sewage and industrial wastes, and a 'storm sewer' which carries storm and surface water. This would be expected to resolve the problems associated with CSOs, but this is not the case. The storm sewers transport water straight to a water course without receiving treatment. This means that sediments and oils picked up from impermeable surfaces such as roads, etc., are transported straight into natural water courses. It is also known for people to tap into the sanitary sewers illegally to allow water from roofing, etc., to be taken away. This increases the loading on the sanitary sewer, and unnecessary spills can occur.

* *Corresponding author: Department of Mechanical Engineering, Cardiff University, Queen's Buildings, The Parade, PO Box 925, Cardiff CF24 0YF, UK.*

1.2 Hydrodynamic vortex separator

An alternative solution to a storage chamber is a hydrodynamic vortex separator (HDVS). HDVSs are used in combined sewers to control the quality of the water being passed to the receiving water course during an overflow event [**2**], where settleable solids can be removed as well as floatable material using a screening system.

The concept of the hydrodynamic vortex separator (HDVS) was first investigated by Smisson in the 1960s [**3**] who aimed to:

> develop a device which could constrain the flow entering to follow a long path through the unit. This would then lengthen the time that gravity aided by other forces due to the rotary motion induced by the kinetic energy of the flow would have to act on the waste water.

This has led to devices that have been developed to provide this increased length. One such device modelled in this work and used by Alkhaddar *et al.* [**1**] to investigate residence times is shown in Fig. 1.

The flow enters the device through a tangential inlet and, owing to the circular geometry of the device, the flow is forced to swirl. The HDVS consists of a number of parts such as the cone and dip plate that induce 'highly stabilized flow patterns' [**3**]. The flow can either pass down through the underflow or up between the dip plate and the baffle plate and over the weir onto the spill way where it then flows out through the overflow [**3**]:

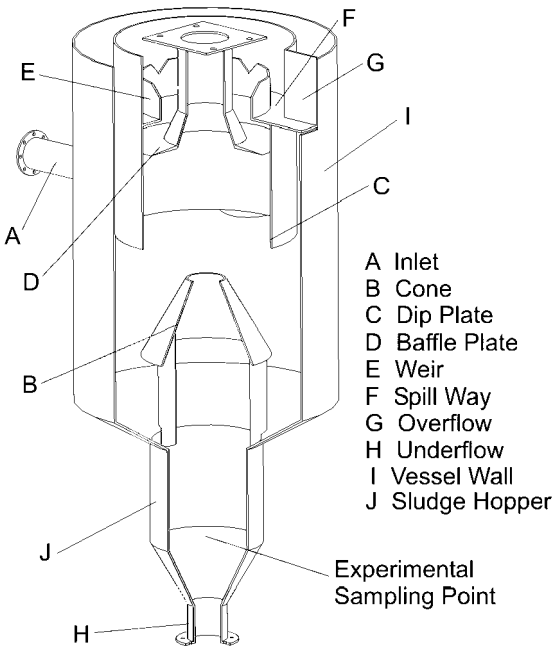

Fig. 1 HDVS studied in this work

> The mean flow pattern observed in an HDVS such as this is a downward helical flow in the outer region and an upward helical flow near the central region. These two spiral flow regimes are separated by a shear zone region and a non-uniform axial profile exists with downward flow along the walls and upward flow along the axis.

The quantity of water passing through the underflow can be controlled using a valve; i.e. the HDVS can be operated with any required flow split which is expressed as a percentage of the inflow, Q_i, such that the flow split is defined as $100Q_b/Q_i$, where Q_b is the base flow which is the flow that removes separated solids.

The flow characteristic of an HDVS will lie somewhere between completely plug flow or completely mixed flow. This allows an HDVS to be used as a contact vessel for disinfection or coagulation/flocculation processes.

In a complete plug flow operating condition, the response to a pulse injection is such that all elements being tracked leave the device at the same residence time, indicated in Fig. 2A. In a completely mixed or backmix flow, the elements of fluid being tracked will leave the device over a range of residence times, shown in Fig. 2B. When a device operates between these characteristics, there is a degree of plug flow that results in an initial peak in a plot monitoring concentration at the outlet, and a degree of mixing where the plot monitoring concentration tails (Fig. 2C). Levenspiel [**4**] discusses this in detail.

Hence, if an HDVS were designed such that there were no internal components and the inlet and outlet were situated opposite one another, then this would most likely result in a device that was dominated by plug flow, where the fluid tends to

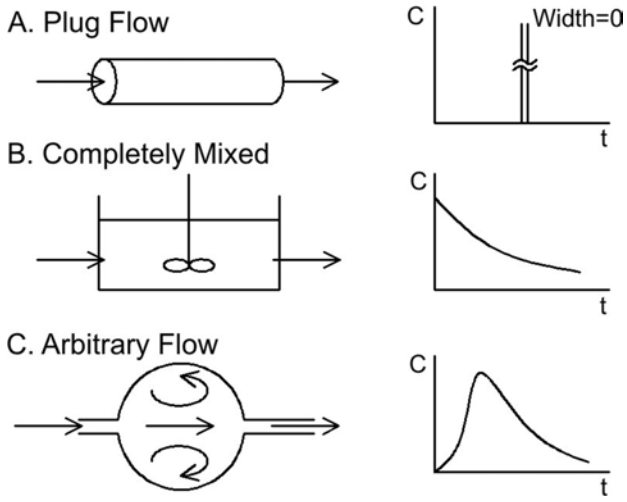

Fig. 2 Concentration versus time plots in response to different types of flow [**4**]

pass straight through the HDVS, with a limited amount of mixing occurring between the outlets. However, for an HDVS such as that shown in Fig. 1, with internal components, the flow patterns will be more complex in that the HDVS aims to increase the length of the path of the fluid through the separator, and hence increase the mean residence time. This would be expected to result in an increased amount of mixing. Further mixing would most likely be achieved by an increase in the turbulence via the use of, say, a paddle to stir the fluid. This, on the other hand, will result in an increased operational and maintenance cost.

A scaling relationship determined through the use of computational fluid dynamics (CFD) for the economical sizing and performance of an HDVS will allow the optimization of added chemicals and will also result in the desired separation efficiency. Before this can be achieved, however, a suitable method using CFD for characterizing the flow of an HDVS must be determined.

2 RESIDENCE TIME

2.1 Residence time applications

Guymer *et al.* [**5**] have investigated the residence time distribution in storage tanks of varying length, and report that the results give 'an insight into the hydraulic processes affecting soluble pollutants as they pass through a storage tank and thus may help to improve the design and operation of storage tanks'.

Boner *et al.* [**6**] report a study in Columbus, Georgia, that compared an HDVS and a conventional mixed basin preceded by a sedimentation basin used for disinfection of the flow from a CSO. It was found that the HDVS was 3 times more effective at disinfection and up to 10 times more effective in removing total suspended solids and other pollutants.

Andoh *et al.* [**7**] have reported the use of an HDVS in removing very fine colloids by the addition of chemicals to aid coagulation and flocculation. An ideal flocculation process is known as 'tapering flocculation' where the hydraulic shear forces decrease as the flow progresses, to reduce the possibility of floc break-up. This flow characteristic is present in an HDVS owing to a faster rotating flow on the outside of the device and a slower moving inner zone [**7**]. For coagulation to occur, the charge state of the colloids is altered by a coagulation aid and allows the colloids to coalesce and form larger agglomerates by flocculation. Flocculation is aided by a flocculant aid which is often a long-chain heavy molecular weight polyelectrolyte. As the flocs grow in size, their settling velocity also increases, so the flocs have a greater chance of being removed from the effluent.

2.2 Experimental determination of residence times

Alkhaddar *et al.* [**1**] have investigated and characterized the residence time distribution of a pilot-scale HDVS, shown in Fig. 1, of 750 mm diameter and operating with a base flow component. This was seen as the first stage in the process of investigating the characteristic and its scaling.

The inlet pipe to the HDVS was a straight pipe extending 24 diameters upstream of the HDVS and a dosing point positioned at 12 diameters upstream. A sampling point was present below the sludge hopper, shown in Fig. 1. The inlet flow was controlled by a gate valve, and flow measurement was made by a calibrated turbine style flowmeter measuring the volume of flow passed. The flowrate was also checked by recording the time taken to fill container of known volume. The study involved the pulse injection of a lithium chloride tracer and, by taking samples from the underflow and overflow for flow splits of 10, 20, 30, and 40 per cent and inlet flowrates of 0.75–6 l/s [**1**], the classical 'method of moments' was used to characterize the residence time distribution of the HDVS [**4**].

The outcome of this work, shown in Fig. 3, found that the device had a 'plug flow mixing characteristic with a degree of non-ideal flow behaviour' [**1**]. This is due to the significant peak of the curves and the long tailing effect where tracer concentration was being measured at 5–6 times the predicted theoretical mean residence time. Hence, the device operates with the arbitrary flow shown in Fig. 2. It was initially thought that the base flow residence time distribution (RTD) curve would peak before the underflow RTD curve. In the results presented here this was not the case. However, it was found that, for a sampling point in the underflow at a slightly different position, the base flow RTD curve did in fact peak before the overflow, and this highlights the importance of the sample location.

It was also found that, generally, as the flow split was increased, the flow at the overflow tended slightly more towards a 'plug flow' regime, and, at the underflow, a 'completely mixed' flow regime. This is reflected in the normalized variance, for which an example is shown in Fig. 4 at a flowrate of 2 l/s. The normalized variance is given by the ratio of the variance of the residence time distribution and the mean residence time squared [**1**]

$$\sigma_\theta^2 = \frac{\sigma^2}{\bar{t}_m^2} \tag{1}$$

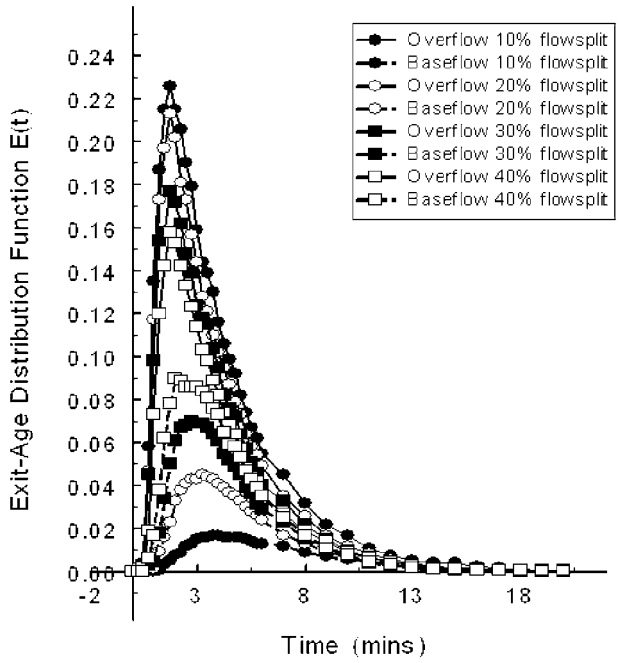

Fig. 3 RTD curves for the HDVS operating at 2 l/s over a range of flow splits [**1**]

where

σ_θ^2 = normalized variance
σ^2 = variance (s^2)
$\bar{t}$ = mean residence time (s)

A normalized variance of 1 indicates a perfectly mixed flow regime, and a value of 0 corresponds to plug flow [**1**]. The slight tendency towards a plug flow regime at the overflow and a mixed flow regime at the underflow could be due to the discharge at the overflow being slower and, hence, less turbulent, so that the mixing decreases. The significant increase in the normalized variance at the underflow is due to the volume of fluid occupying the sludge hopper, shown in Fig. 1, becoming more active and, therefore, more turbulent, and this aids the mixing process.

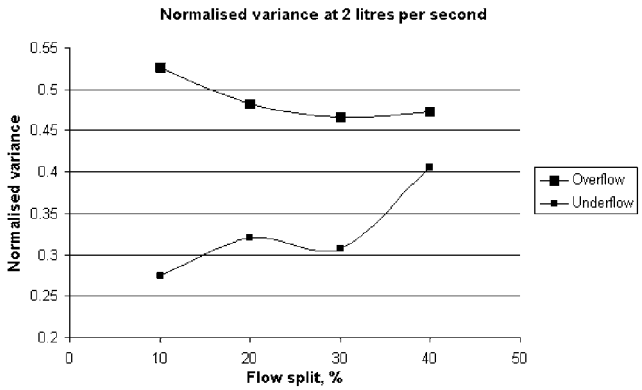

Fig. 4 Normalized variance at various flow splits at 2 l/s

2.3 Determination of the residence time using computational methods

The determination of residence time distributions using numerical methods has been attempted previously using alternative methods to those presented in this paper. One of these methods is by introducing a second species which acts as the tracer and this species can be monitored at the outlet and an RTD curve plotted. Sherwin and Ta [**8**] used this to investigate short-circuiting in an anaerobic zone consisting of a baffle plate and two mixers. Ta and Brignal [**9**] used the same technique to study the residence time of a storage reservoir. Contours of species concentration can also be viewed within the domain being modelled which will reveal the path of the fluid through the system. The author has found in using this technique, however, that computation of the flow and turbulence equations is required throughout the entire solution, resulting in a substantial and undesired increase in processing time.

2.4 Theoretical analysis

Alkhaddar *et al.* [**10**] have developed a 'combined mathematical' model for predicting the residence time distribution of an HDVS operating without a base flow component. The approach to this model was through the 'axial dispersion model' and the 'tanks in series model' as the shape of the residence time curve could not be represented accurately by either model on its own. The model was developed by assuming that the HDVS being modelled could be described by three continuously stirred tank reactors (CSTRs), connected in series and all having ideal CSTR behaviour. It was also assumed that one of these tanks could exchange with a slow mixing zone, i.e. the fluid within the sludge hopper, shown in Fig. 1, represented by a fourth tank, and that the inlet and outlet could be connected by a bypass with an adjustable flowrate, hence allowing short-circuiting.

It was found that, with increased influent flowrate, bypassing increases and the slow mixing volume decreases [**10**]. Thus, the boundary conditions selected for the model, in particular the conditions for the fourth tank which allows short-circuiting, must be based on knowledge of experimental results.

2.5 HDVS scaling

Tyack and Fenner [**11**] used a scaling protocol to characterize the residence time of two HDVSs, one 0.3 m in diameter, which will be referred to as the 'model', and another 1.6 m in diameter, which will be referred to as the 'prototype'. Residence time data were collected using lithium chloride as a tracer, injected as a pulse. The scaling protocol was derived in the following manner.

Considering Buckingham's π theorem, the relevant parameters were chosen by considering the characteristics of the residence time, the separator, the fluid flow, and the liquid. Table 1 shows the parameters related to each of these characteristics.

Applying Buckingham's π theorem with Q, D, and ρ as the repeating variables yields the equation

$$\text{Residence time} = f\left(\frac{Qt}{D^3}, \frac{d}{D}, \frac{h}{D}, \frac{D^5 g}{Q^2}, \frac{H}{D}, \frac{Q\rho}{D\mu}, \frac{D^4\tau}{\rho Q^2}\right) \quad (2)$$

The dimensionless group $(tQ)/D^3$ is the ratio of the actual to the theoretical overflow rate, and $Q^2/(D^5 g)$ is the Froude number. If the two HDVSs used are geometrically identical, and if t is set as $\bar{t}$, the mean residence time, then, considering the first term in equation (2)

$$\frac{Q_{\text{model}}\bar{t}_{\text{model}}}{D^3_{\text{model}}} = \frac{Q_{\text{prototype}}\bar{t}_{\text{prototype}}}{D^3_{\text{prototype}}} \quad (3)$$

'If Froude numbers are chosen to scale the flows, as used by previous researchers' [**11**], it can be shown that

$$\frac{Q_{\text{model}}}{Q_{\text{prototype}}} = \left(\frac{D_{\text{model}}}{D_{\text{prototype}}}\right)^{5/2} \quad (4)$$

Let

$$L_{\text{r}} = \frac{D_{\text{prototype}}}{D_{\text{model}}} \quad (5)$$

Table 1 Relevant parameters related to each characteristic

Characteristic	Relevant parameters
Residence time	t, D, h
Separator	D, d, h, τ
Fluid flow	Q, g, H, τ
Liquid	ρ, μ

t = residence time (s); D = diameter of the separator body (m); h = height of the separator body (m); d = inlet pipe diameter (m); τ = shear stress between the separator and fluid (N/m^2); Q = through flowrate (m^3/s); g = acceleration due to gravity (m/s^2); H = head loss across the separator (m); ρ = fluid density (kg/m^3); μ = fluid viscosity (kg/m s).

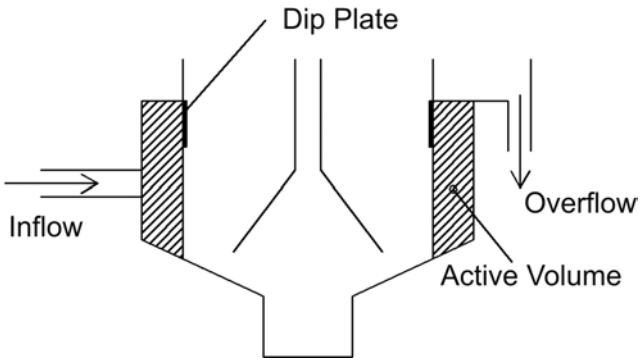

Fig. 5 Schematic of the 'active' volume

Then, rearranging equation (3) to make $\bar{t}_{\text{prototype}}$ the subject, and substituting equations (4) and (5), gives the scaling protocol

$$t_{\text{prototype}} = L_{\text{r}}^{0.5} t_{\text{model}} \quad (6)$$

Tyack *et al.* defined the theoretical time to peak concentration, t_{R}, as

$$t_{\text{R}} = \frac{V}{Q} \quad (7)$$

where V is the volume of flow within the HDVS, so that

$$\frac{\bar{t}_{\text{model}}}{t_{\text{Rmodel}}} = \frac{\bar{t}_{\text{prototype}}}{t_{\text{Rprototype}}} \quad (8)$$

Tyack *et al.* found that theoretical and actual 'time to peak' concentrations coincide only when the 'active' volume of flow is considered, shown in Fig. 5, which is 'the volume between the outside wall of the separator body and the vertical line located at the position of the dip-plate' [**11**].

Figure 6 shows the mean residence times after scaling the 0.3 m model tests up to the 1.6 m

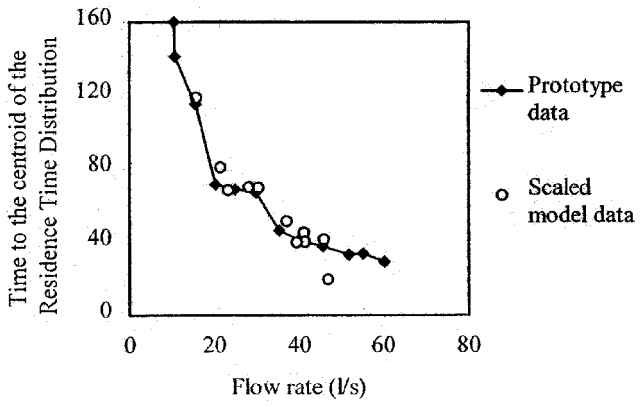

Fig. 6 Result of scaling the residence time data using the scaling protocol and scaling the flowrates using the Froude number [**11**]

prototype tests using the scaling protocol [equation (6)] and the Froude number to scale the flows [equation (4)]. As can be seen, 'the fit of the scaled model data to the prototype is very good' [**11**].

3 COMPUTATIONAL FLUID DYNAMICS

3.1 Introduction

The most efficient simulation method for investigating scaling effects is through the use of computational fluid dynamics (CFD), which is used in a variety of engineering fields, such as the microprocessor industry, the automotive industry, and the power industry. In this work, the CFD code Fluent was used. When using CFD, the general procedure is as follows:

(a) create the geometry in which the fluid is to be modelled;
(b) apply a mesh to which the finite difference algorithms will be applied;
(c) apply boundary conditions such as fluid velocities, etc.;
(d) solve the fluid transport equations;
(e) post-process, i.e. examine the results.

It is also possible when using Fluent to write a user-defined function (UDF) which is a subroutine written in the C programming language and can be used for custom calculations, boundary conditions, or material properties. This feature gives the user greater flexibility.

3.2 Grid set-up and boundary conditions

The inlet pipe to the HDVS in Fig. 1 was offset slightly in order to prevent overskewed cells at the point where the inlet pipe is joined to the HDVS vessel wall as this would result in appreciable error and possible convergence problems during computation of the flow. The walls forming the dip plate, baffle plate, cone, etc., were zero thickness, owing to the very fine cells that would result from modelling the actual thickness of these components.

A mesh was constructed, shown in Fig. 7, which comprised 745 471 cells, and the geometry was split such that a finer mesh was present along the side of the dip plate (A) owing to the very narrow gap between the baffle plate and the dip plate where all the fluid leaving the device through the overflow has to pass. It was believed that a finer mesh here would yield a more accurate flowfield in relation to the fluid flowing up and out of the device. The faces forming the 'V' notches in the weir (B) also had a finer mesh. In general it was also ensured that a minimum of six cells were present between two faces that formed a channel, e.g. between the weir and baffle plate (C), or between the dip plate and the walls of the vessel (D), and in the underflow. This was to ensure that a crude boundary layer could

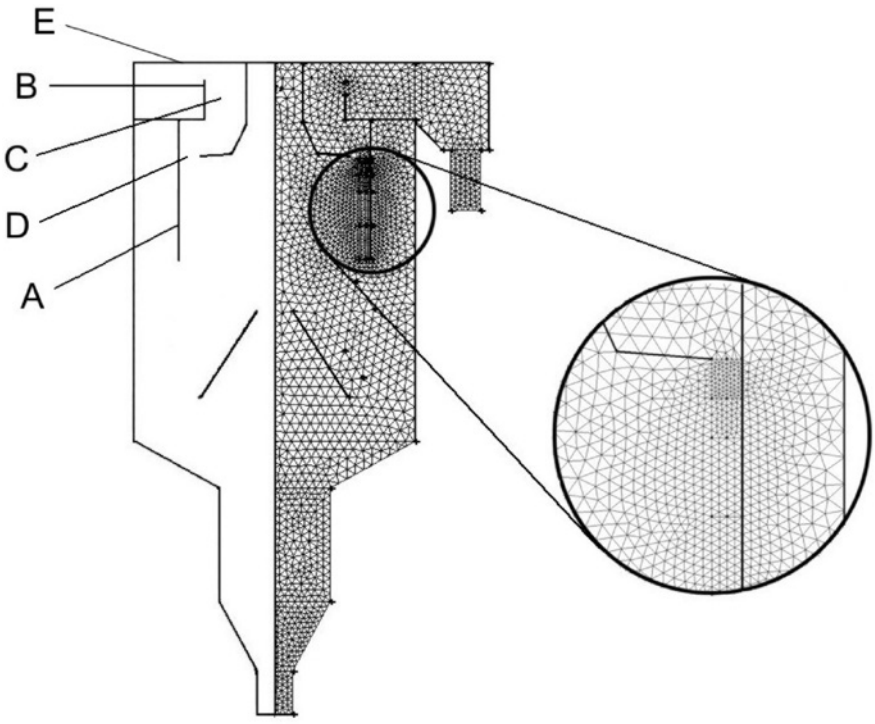

Fig. 7 A schematic of the mesh used to model the HDVS

be represented while also allowing for fluid to pass through the cells in the centre of the channel. Owing to the geometry of the HDVS, these requirements utilized a large number of cells, leaving few cells to refine other regions without increasing processing time even further.

The free surface between the water and air was modelled as a frictionless wall (Fig. 7, E), to avoid using a multiphase model for computing the flow transport equations. The overflow was specified as a pressure outlet for which all the flow quantities excluding pressure (except in special circumstances not present in this work) were extrapolated from the interior. The underflow was specified as a velocity inlet for which a negative velocity was applied in order to obtain the required flow split. A steady state solution was achieved for all the models using the highest-order turbulence model which closes the Reynolds-averaged Navier–Stokes equations by solving transport equations for the Reynolds stresses. This is known as the Reynolds stress model.

In predicting the residence times using CFD, two approaches were taken:

(a) a discrete phase approach whereby particles are injected;
(b) a user-defined scalar (UDS).

In using a UDS, there are four ways in which it may be applied to investigate the residence time characteristics of a device. The first is a pulse input to produce a plot known as a C curve which is a function of the concentration of UDS in the exit stream with time. This can be used to produce an E curve known as an exit age distribution function where $E\,\mathrm{d}t$ is the fraction of material in the exit stream with an age between t and $t + \mathrm{d}t$. A second method is a step input to produce a plot known as an F curve which is a function of the fraction of tracer concentration in the exit stream with time, where the fraction of material in the exit stream is in relation to the concentration in the inlet stream. The entire device can also be filled with UDS and drained to determine the internal age distribution, known as an I curve, where $I\,\mathrm{d}t$ is defined in the same way as $E\,\mathrm{d}t$. The final use of a UDS in characterizing a mixing device is as a source to calculate the mean residence time.

4 DISCRETE PHASE APPROACH

After solving the flow of water into the HDVS, 1 μm neutrally buoyant discrete particles was injected into the system using stochastic tracking as the turbulent dispersion model. The mean residence time and RTD curve could then be determined from a report produced for the particles that leave through the outlets.

Figure 8 shows an RTD curve produced from particle tracking by plotting the number of particles that leave the outlet in a time step decided by the user. The smaller the time step, the more accurate is the plot but the greater is the number of particles that have to be tracked in order to make the curve

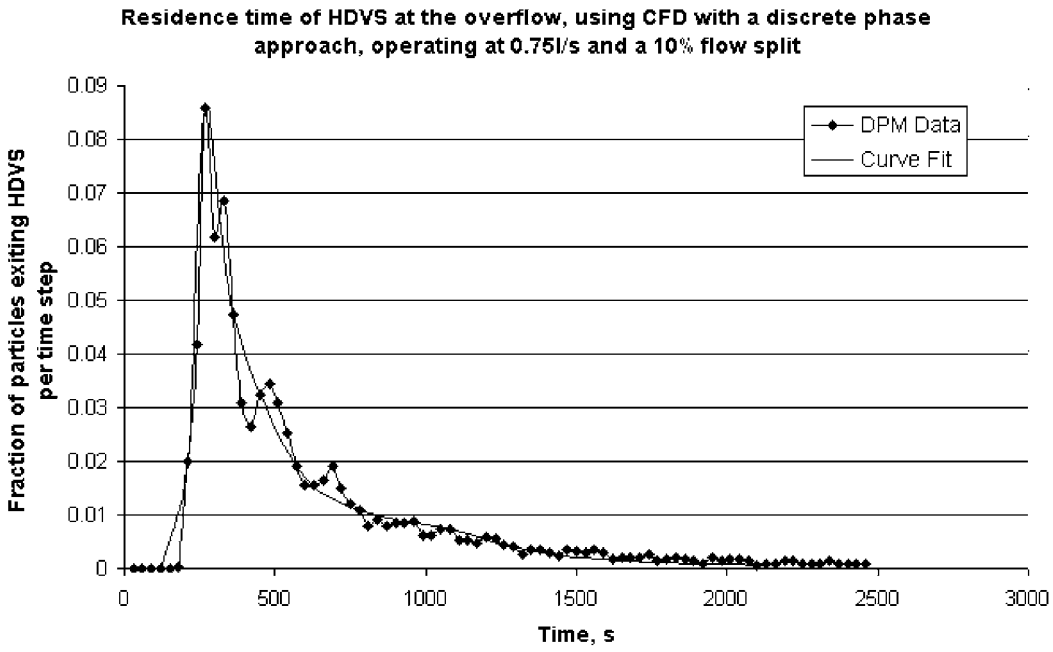

Fig. 8 RTD curve for the HDVS using a discrete phase model approach

as smooth as possible, and this results in a greater, undesired, processing time. Although 10 000 particles are injected into the system, the plot in Fig. 8 is not smooth, which makes it harder to characterize the HDVS using CFD. A curve was fitted to the data, shown in Fig. 8, which provides a trade-off between a high processing time and accuracy.

When using a discrete phase model there is a calculation for drag on the particle; ideally, the particle will always have the same velocity as the fluid. A particle with a diameter of zero cannot be specified so that the particle follows the fluid perfectly. The particle trajectory is given by the equation [**12**]

$$\frac{\mathrm{d}u_\mathrm{p}}{\mathrm{d}t} = F_\mathrm{D}(u - u_\mathrm{p}) + \frac{g(\rho_\mathrm{p} - \rho)}{\rho_\mathrm{p}} \tag{9}$$

where

u_p = particle velocity (m/s)
t = time (s)
u = fluid velocity (m/s)
ρ = fluid density (kg/m^3)
ρ_p = particle density (kg/m^3)
u = fluid velocity (m/s)
u_p = particle velocity (m/s)
g = acceleration due to gravity (m/s^2)
$F_\mathrm{D}(u - u_\mathrm{p})$ = drag force per unit particle mass

The drag force is defined by the equation

$$F_\mathrm{D} = \frac{18\mu}{\rho_\mathrm{p} d_\mathrm{p}^2} \frac{C_\mathrm{D} Re}{24} \tag{10}$$

where

μ = fluid viscosity (kg/m s)
d_p = particle diameter (m)
C_d = drag coeffcient
Re = particle Reynolds number

It can be seen that the units of each of the three terms in equation (9) are m/s^2, i.e. the force per unit particle mass. The particle mass is a function of the particle diameter, and thus, when the particle has a diameter of zero, equation (9) reduces to zero. The Fluent software therefore classes a particle with a diameter of zero as a particle that has evaporated.

Owing to computational power, only a relatively small finite number of particles can be tracked; ideally, the same number of particles would be monitored as ions produced in the tracer solution. Particles that get close to walls can get stuck on account of boundary layer effects, thus increasing the residence time of the particle which has a significant impact on the mean owing to the small number that can be tracked. It was found that, for the plot in Fig. 8, a 96 per cent mass recovery was achieved within 5.19 h, in spite of a mean residence time of 14.9 min, owing to particles that had got stuck in the device. Had every single particle been recovered, given an even higher run time, then the mean residence time would also have been higher.

These problems were resolved, with little improvement in results, firstly through the use of a user-defined function (UDF) to assign the velocity of the fluid to the velocity of the particle. Fluent Inc. reported that, once the particle position has been updated, the velocity is assigned to the particle by the UDF, and then the velocity of the particle is updated by the Fluent formulation. Hence, the authors believe that this UDF was unsuccessful, most likely owing to the way in which the Fluent solver is structured. A UDF was also used to prevent the particle getting close to the walls, a feature known as saltation.

5 USER-DEFINED SCALAR APPROACH

The user-defined scalar approach is essentially taken from the local mean age of air developed for use in modelling heating, ventilation, and air conditioning (HVAC) but which is shown here also to be applicable to the analysis of hydraulic systems.

5.1 UDS theory

For an arbitrary scalar, ϕ_k, the transport equation to be solved is given by the equation [**12**]

$$\frac{\partial \rho \phi_k}{\partial t} + \frac{\partial}{\partial x_i}\left(\rho u_i \phi_k - \Gamma_k \frac{\partial \phi_k}{\partial x_i}\right) = S_{\phi_k} \tag{11}$$

where

Γ_k = diffusion coeffcient (m^2/s)
S_{ϕ_k} = source term

This transport equation is solved for a UDS and allows the fluid flowing into the HDVS to be marked in a way such that the UDS acts as a tracer. The diffusivity of the UDS is defined as being the same as the fluid flowing through the HDVS, and in a turbulent flow it is a function of the binary diffusivity, the turbulent and laminar viscosity,

and the turbulent Schmidt number, given in the equation [**12**]

$$\text{Diffusivity} = D_b\rho + \frac{\mu_L + \mu_T}{Sc_t} \tag{12}$$

where

D_b = binary diffusivity (m^2/s)
μ_L = laminar viscosity (kg/m s)
μ_T = turbulent viscosity (kg/m s)
Sc_t = turbulent Schmidt number

The turbulent Schmidt number is defined as

$$Sc_t = \frac{\mu_T}{\rho D_t} \tag{13}$$

where D_t is the turbulent diffusivity (m^2/s).

The mean residence time of a fluid is solved such that the fluid enters the control volume, in this case the HDVS, where it is split into finite control volumes. At time t the mass flowrate of fluid into a cell is $\dot{m}$, such that the value of the scalar when it enters the cells is $\dot{m}t$. When the fluid leaves the cell, its age will have increased by Δt such that the value of the scalar when it leaves the cell is $\dot{m}(t + \Delta t)$ (Fluent Inc., 2003, personal communication). In order to find the time at which the fluid leaves, a source term is required equivalent to

$$S_{\phi_k} = \frac{\dot{m}\Delta t}{V} \tag{14}$$

where

$\dot{m}$ = mass flow rate (kg/s)
V = volume (m^3)

The source term is divided by the cell volume since it is applied on a volumetric basis. However, the time is not known, and nor is the mass flowrate through the cell; hence, by considering the following relationships, the source term is simplified

$$\dot{m} = \rho A u = \rho \dot{V} \tag{15}$$

where

A = area (m^2)
$\dot{V}$ = volumetric flowrate (m^3/s)

Rearranging equation (15) gives

$$\dot{V} = \frac{\dot{m}}{\rho} \tag{16}$$

and since

$$\Delta t = \frac{V}{\dot{V}} \tag{17}$$

then substituting equation (16) into equation (17) gives

$$\Delta t = \frac{V\rho}{\dot{m}} \tag{18}$$

Now, substituting (18) into (14) gives

$$S_{\phi_k} = \rho \tag{19}$$

A detailed discussion and mathematical derivation is given by Roos [**13**].

The source term is very convenient, particularly for incompressible fluids at a constant temperature and pressure, as the density is also constant. The mean residence time can then be evaluated using the Fluent software. Using the transient solver, the response to different inputs can be monitored to yield a *C*, *F*, and *I* curve.

5.2 UDS results

5.2.1 Mean residence time

Figure 9 shows experimentally determined mean residence times by Alkhaddar *et al.* [**1**], and predicted mean residence times using CFD for the HDVS operating at 2 l/s at flow splits between 10 and 40 per cent. Clearly, the user-defined scalar matches the experimental data the closest. Similar plots were made for all the operating conditions that were reported by Alkhaddar *et al.* [**1**], i.e. flowrates of 0.75, 1, 2, 4, and 6 l/s and with each flowrate operating at four different flow splits between 10 and 40 per cent. It was found that the mean error when using the discrete phase was of the order of 18 per cent, whereas the mean error using the UDS was of the order of 11 per cent. In general, the DPM approach tended to underpredict the mean residence time. It is thought that this may be due to injecting only 10 000 particles. It has been found from a study at the highest flowrate of 6 l/s that, if the number of particles injected exceeds 30 000, then the error in the mean residence time prediction is of the order of 4 per cent, compared with 20 per cent with an injection of 10 000 particles (the UDS approach at this particular flowrate has an error of

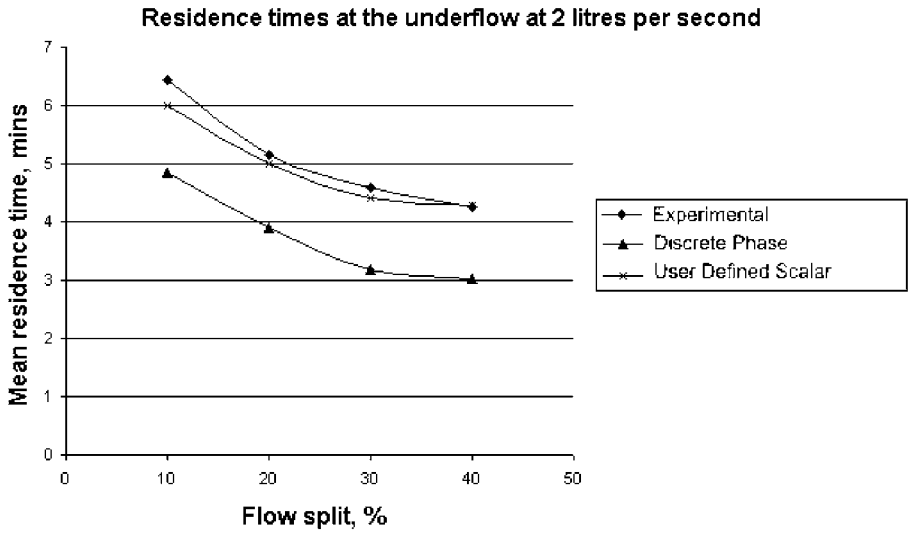

Fig. 9 Mean residence times predicted using CFD using a discrete phase model and a user-defined scalar

6 per cent). However, processing the trajectory of 30 000 particles is time consuming, especially when the mean residence time is high. The quantity of data also becomes increasingly harder to process using a spreadsheet package such as Excel®.

Table 2 shows the mean residence times determined using a UDS, at the overflow and underflow at 2 l/s at four flow splits. Using the UDS, contours of mean residence time can also be plotted, shown in Fig. 10, which highlights 'dead' regions where high contact times occur, such as the region enclosed by the baffle plate, and regions of low residence time, such as the outer regions of the main vessel where the flow circulates straight after entering through the inlet. This can be compared with the plot of contours of velocity magnitude also in Fig. 10 which is for the same operating conditions and can be used for estimating the regions where the mean residence time will be low or high. On the outer part of the vessel the velocity is high after the fluid has entered the HDVS through the inlet. In this region the mean residence time is low. In the region at the top of the HDVS surrounded by the baffle plate the velocity is very low, and here a high residence time would be expected owing to the fluid being stagnant; this can be seen to be true in Fig. 10.

Table 2 Mean residence times of the HDVS at 2 l/s

	Flow split (%)			
	10	20	30	40
Mean residence time, overflow (s)	239.5	240	241	246.5
Mean residence time, underflow (s)	365	304	275	260

Figure 11 shows the ratio of the UU Reynolds stresses and the mean inlet velocity squared. This is the fluctuating velocity component in the direction perpendicular to the contour plane in Fig. 10. The higher the fluctuating velocity component, the greater is the amount of mixing that would be expected to occur in a region.

It can be seen from Fig. 11 that the highest fluctuating components exist around the circumference of the main vessel of the HDVS. This would be expected from the higher velocity that exists in the same region in Fig. 10, and also the higher shear where the fluid is adjacent to a wall. In spite of the fluctuating components being very low, this feature would be expected to assist in some mixing and prevent scaling of contaminants on the HDVS vessel wall. The flow pattern shown in Figs 10 and 11 is in agreement with Andoh and Cook [**7**] who report that the flow patterns in an HDVS provide 'tapering flocculation' where the shear forces decrease as the flow progresses through the HDVS and, hence, the possibility of floc break-up decreases as the residence time increases.

5.2.2 HDVS RTD characterization

Figure 12 shows a family of exit age distribution curves for a pulse input, determined using a UDS, for the HDVS operating at 2 l/s over a range of flow splits. For the data in Fig. 12, a mass recovery of 99.9 per cent was achieved by 1100 s. Although the processing time for a pulse input is longer than for calculating the mean, a much smoother and accurate curve is produced compared with the discrete phase method shown in Fig. 8. The run time could be reduced by using a larger time

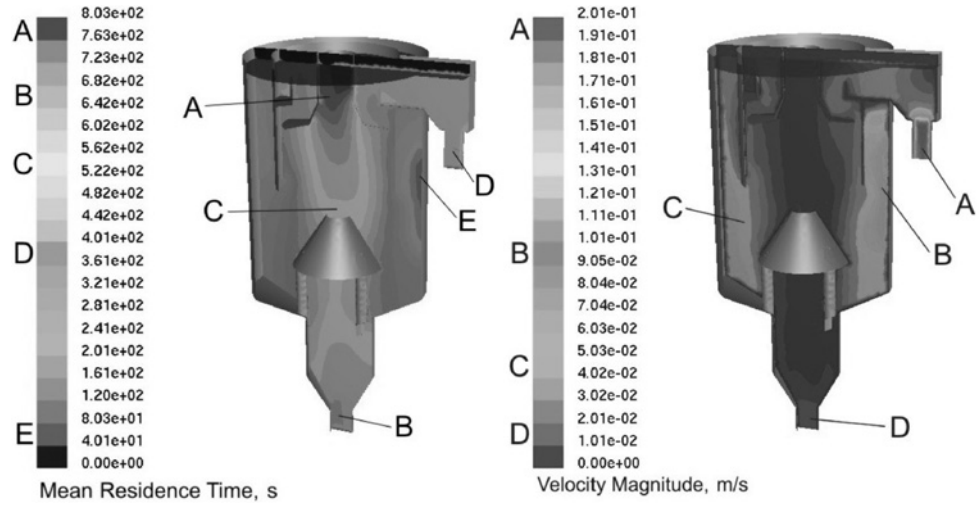

Fig. 10 Contours of mean residence time and velocity magnitude

step, or terminating when the concentration of UDS drops below a value deemed by the user to be acceptable. Although Alkhadar *et al.* [**1**] thought that the base flow would peak before the overflow, the CFD results show otherwise. In contrast to the experimental methods where a point in the outlet is monitored, using CFD the average concentration of the UDS over the outlet surface is monitored. The exit age distribution curves in Fig. 12 show how the RTD curve for the underflow peaks after the overflow, which would be expected from the results for mean residence time in Table 2, where the mean residence time for the underflow is greater than for the overflow. It can be seen, however, that, as the flow split increases, the mean residence time for the underflow decreases and increases for the overflow. This is also evident in the results published by Alkhaddar *et al.* [**1**] for the underflow, but is not as clear in the overflow. This would imply that the amount of short-circuiting increases for the outlet with a greater flow split. An advantage with CFD is that the surface of the outlet can be monitored at time intervals specified by the user. During experimentation by Alkhaddar *et al.* [**1**], online sampling was not available and only a limited number of samples, from a point shown in Fig. 1, could be

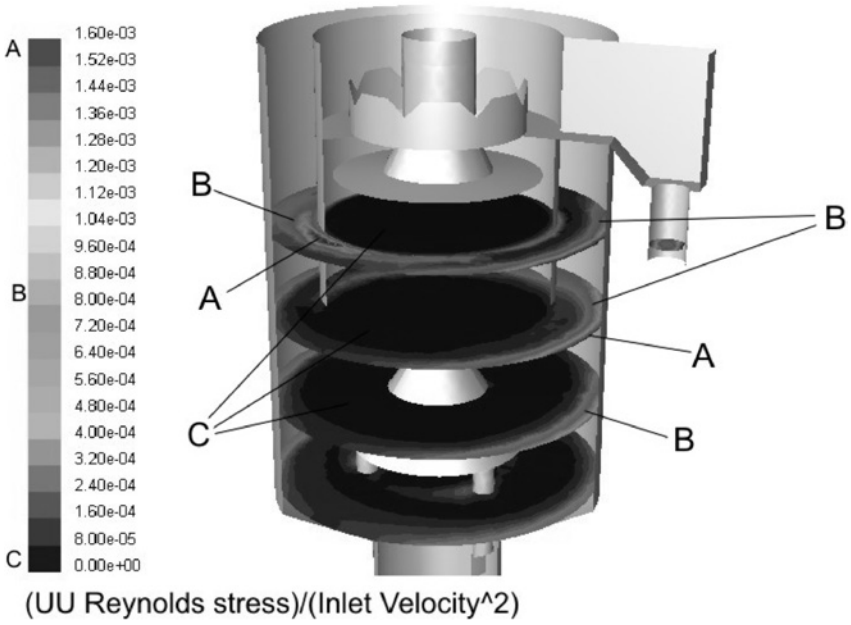

Fig. 11 Contours of fluctuating components

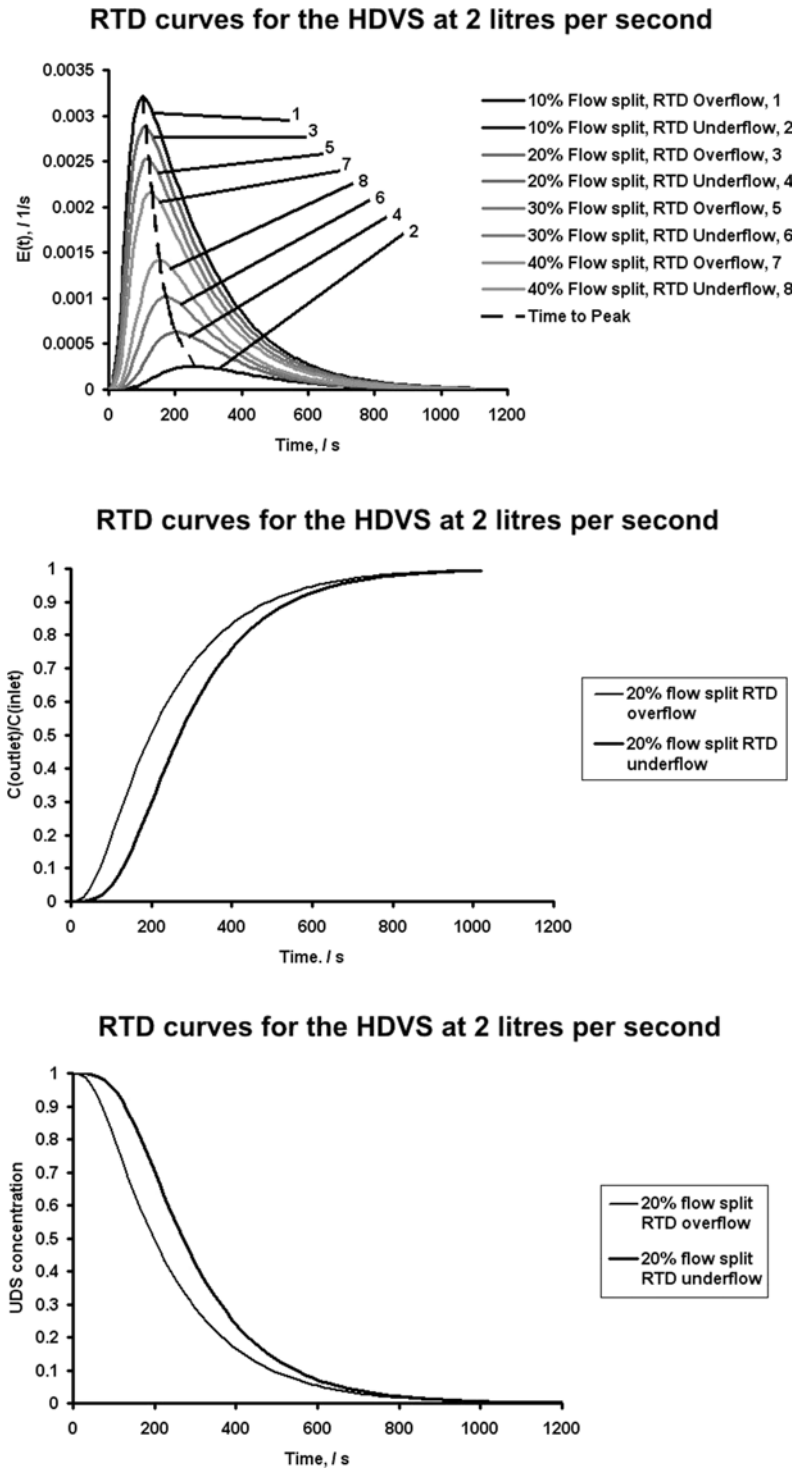

Fig. 12 RTD curves for the HDVS

taken, which may be why the trend in the time to peak for the overflow is not very clear.

Using a UDS, it is also possible to simulate the response to a step input. Figure 12 shows the plot of an F curve using a UDS. As expected, owing to the mean residence time in the overflow being shorter than in the underflow, the concentration of UDS in the overflow increases faster than in the underflow. Short-circuiting in the HDVS is indicated by a sharp rise in the curves, and mixing is indicated by the way in which the curves plateau as the concentration of UDS in the outlets approaches 1;

i.e. the steeper the curve, the less mixing that has occurred. Figure 13 shows four contour plots of tracer concentration in response to a pulse input. At 15 s the onset of flow of UDS around the circumference of the HDVS can be seen, and at 75 s the concentration of UDS is greatest around the circumference of the HDVS vessel walls. By 285 s it is clear that mixing is occurring as contours of UDS greater than zero are present throughout the HDVS, and by 585 s the tracer is almost completely mixed, and this is ideal for chemical disinfection or flocculation.

Again, using a UDS it is possible to determine the internal age distribution function and produce an *I* curve, shown in Fig. 12. Once more, plug flow characteristics are indicated by the steep gradient between 50 and 250 s in the overflow, and mixing characteristics are evident where the plot starts to plateau towards a concentration of 0 in the outlet. The concentration of UDS in the overflow decreases faster than in the underflow, which implies that there is short-circuiting towards the overflow for the configuration modelled.

6 DISCUSSION

Two techniques have been compared in order to find the mean residence time of an HDVS. The first is where neutrally buoyant particles are injected and the mean residence time is found from a report of the time at which each particle leaves through the outlet. The second is where a UDS is introduced which compares closely with experimental data, and, although a plot of the number of particles that leave through the outlet in a time step can be similar to a *C* curve when using the discrete phase approach, the UDS produces a *C* curve that is smoother, and hence

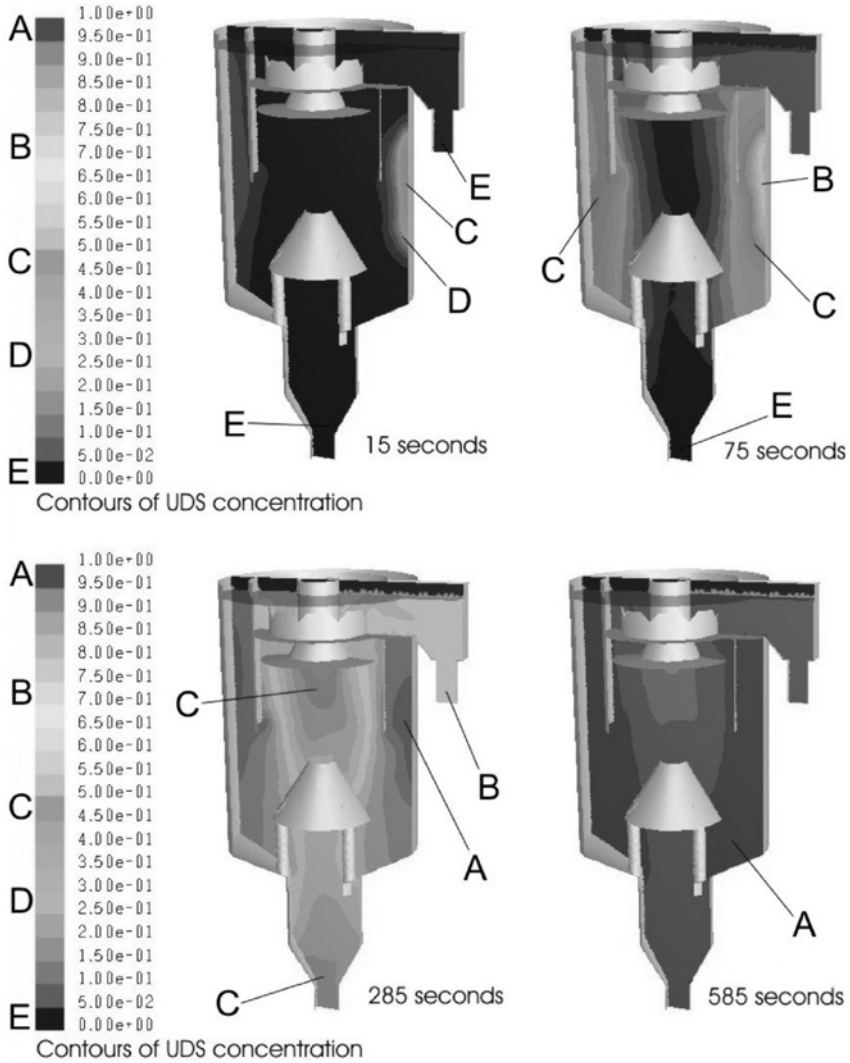

Fig. 13 Contours of tracer concentration in response to a step input at 2 l/s and a 20 per cent flow split

easier to interpret. An added advantage of the UDS is that a contour plot of mean residence time can be viewed to study regions of high and low residence time within the device, which could then be used to make a decision on design modifications to increase or decrease the residence time in a particular region of the HDVS as required. The UDS also allows the characterization of a HDVS by producing *F*, *I*, and *E* curves. The HDVS has been characterized using all these inputs. In agreement with the work by Alkhaddar *et al.* [**1**], the device can be seen to have a certain amount of plug flow, which is seen, for example, in the sudden rise in mass fraction at the outlets in the exit age distribution plots in Fig. 12, but also a certain amount of mixing owing to the tailing effect in both the exit age distribution plots and the internal age distribution plot in Fig. 12. Thus, the HDVS studied has an arbitrary flow regime which is shown in Fig. 2, C. Figure 13 shows contours of UDS in response to a step input and clearly shows the mixing of the tracer in the device with time. Figure 11 shows that mixing can be expected around the circumference of the HDVS vessel walls, which is desirable when disinfection or chemical-assisted flocculation is required, and, although there is very little mixing in the centre of the HDVS, Fig. 10 shows that here there is a high residence time, which compensates for little mixing as the fluid has a high contact time. A UDS can thus be used in order to find a scaling law for fluid residence time in an HDVS. This paper outlines how this may be carried out, and the scaling protocol described can be used to determine its suitability, particularly for an HDVS that is much larger than 1.6 m (separators as large as 11 m in diameter have been installed at a site in Columbus, Georgia). A scaling law will allow an efficient use of reagents in order to achieve the required level of disinfection or flocculation.

7 CONCLUSION

A method for characterizing an HDVS using a user-defined scalar has been adapted from that for determining the mean age of air in HVAC. The technique has been successfully validated against experimental data and compared with a second technique using particles. The technique using a UDS has advantages over the discrete phase approach in that it is faster in determining the mean residence time, generally more accurate, and involves less manual processing. The UDS can also be used to produce a *C*, *E*, *F*, and *I* curve, all of which are very useful for determining the flow behaviour in an HDVS. This technique can be applied to predicting scaling laws for residence times in HDVSs.

ACKNOWLEDGEMENTS

The authors wish to thank Hydro International plc and EPSRC for funding and support.

REFERENCES

1 **Alkhaddar, R. M., Higgins, P. R., Phipps, D. A.,** and **Andoh, R. Y. G.** The residence time distribution of prototype hydrodynamic vortex separator operating with a baseflow component. 8ICUSD, 30 August–3 September 1999, pp. 18–25.

2 **Andoh, R. Y. G.** and **Saul, A. J.** The use of hydrodynamic vortex separators and screening systems to improve water quality. *Water Sci. and Technol. (IWA)*, 2003, **47**(4), 175–183.

3 **Andoh, R. Y. G.** and **Smisson, R. P. M.** High rate sedimentation in hydrodynamic separators. 2nd International Conference on *Hydraulic Modelling Development and Application of Physical and Mathematical Models*, 1993, pp. 341–358.

4 **Levenspiel, O.** *Chemical Engineering*, 1962 (John Wiley, New York).

5 **Guymer, I., Shepherd, W. J., Dearing, M., Dutton, R.,** and **Saul, A. J.** Solute retention in storage tanks. 9th International Conference on *Urban Drainage*, 8–11 September 2002.

6 **Boner, M. C., Hides, S. P.,** and **Turner, B. G.** High rate treatment of combined sewer overflows in Columbus, Georgia. In Proceedings of 6th International Conference on *Urban Storm Drainage*, 12–17 September 1993, pp. 1671–1676.

7 **Andoh, R. Y. G.** and **Cook, A. P.** The Eff-Pac^{TM} process for industrial wastewater treatment. Filtech Conference, Karlsruhe, 1995, pp. 173–189.

8 **Sherwin, C.** and **Ta, C. T.** Investigation of anaerobic zone short circuiting using computational fluid dynamics. *Water Sci. and Technol.*, 2002, **46**(4, 5), 333–338.

9 **Ta, C. T.** and **Brignal, W. J.** Application of computational fluid dynamics technique to storage reservoir studies. *Water Sci. and Technol.*, 1998, **37**(2), 219–226.

10 **Alkhaddar, R. M., Cheong, C. H., Phipps, D. A., Andoh, R. Y. G., James, A.,** and **Higgins, P.** The development of a mathematical model for the prediction of the residence time distribution of a hydrodynamic separator. *Novatech*, 2001, 835–842.

11 **Tyack, J. N.** and **Fenner, R. A.** The use of scaling laws in characterising residence time in hydrodynamic separators. In Proceedings of 2nd International Conference on *The Sewer as a Physical, Chemical and Biological Reactor*, Aalborg, Denmark, 25–28 May 1997.

12 *Fluent 6.1 Documentation*, 2003 (Fluent Inc., Lebanon).

13 **Roos, A.** On the effectiveness of ventilation. PhD thesis, Eindhoven University of Technology, Eindhoven, The Netherlands, 1999.

APPENDIX

Notation

A	area (m^2)
CFD	computational fluid dynamics
CSO	combined sewer overflow
CSTR	continuously stirred tank reactor
C_d	drag coefficient
d	inlet pipe diameter (m)
d_p	particle diameter (m)
D	diameter of the HDVS (m)
D_b	binary diffusivity (m^2/s)
D_t	turbulent diffusivity (m^2/s)
g	acceleration due to gravity (m/s^2)
h	height of the HDVS body (m)
HDVS	hydrodynamic vortex separator
H	head loss (m)
$\dot{m}$	mass flowrate (kg/s)
Q	flowrate (m^3/s)
RTD	residence time distribution
Re	particle Reynolds number
S_{ϕ_k}	source term (kg/m^3)
Sc_t	turbulent Schmidt number
t	time (s)
t	residence time (s)
$\bar{t}$	mean residence time (s)
Δt	time step (s)
u	fluid velocity (m/s)
u_p	particle velocity (m/s)
UDF	user-defined function
UDS	user-defined scalar
V	volume of flow within the HDVS (m^3)
$\dot{V}$	volumetric flowrate (m^3/s)
Γ_k	diffusion coefficient (m^2/s)
μ	fluid viscosity (kg/m s)
μ_L	laminar viscosity (kg/m s)
μ_T	turbulent viscosity (kg/m s)
ρ	fluid density (kg/m^3)
ρ_p	particle density (kg/m^3)
σ_θ^2	normalized variance
σ^2	variance (s^2)
τ	shear stress between the separator and fluid (N/m^2)